IEEE Access
Multidisciplinary ⋮ Rapid Review ⋮ Open Access Journal

Received April 15, 2021, accepted April 26, 2021, date of publication April 28, 2021, date of current version May 10, 2021.

Digital Object Identifier 10.1109/ACCESS.2021.3076410

Hybrid Wavelet Stacking Ensemble Model for Insulators Contamination Forecasting

STÉFANO FRIZZO STEFENON[1], (Graduate Student Member, IEEE), MATHEUS HENRIQUE DAL MOLIN RIBEIRO[2,3], ADEMIR NIED[1], (Member, IEEE), VIVIANA COCCO MARIANI[4,5], LEANDRO DOS SANTOS COELHO[2,4], VALDERI REIS QUIETINHO LEITHARDT[6,7], (Member, IEEE), LUIS AUGUSTO SILVA[8], AND LAIO ORIEL SEMAN[9]

[1]Electrical Engineering Graduate Program, Electrical Engineering Department, Santa Catarina State University (UDESC), Joinville 89219-710, Brazil
[2]Industrial and Systems Engineering Graduate Program (PPGEPS), Pontifical Catholic University of Paraná (PUCPR), Curitiba 80215-901, Brazil
[3]Department of Mathematics, Federal University of Technology–Parana (UTFPR), Pato Branco 85503-390, Brazil
[4]Department of Electrical Engineering, Federal University of Paraná (UFPR), Curitiba 81531-980, Brazil
[5]Mechanical Engineering Graduate Program (PPGEM), Pontifical Catholic University of Paraná (PUCPR), Curitiba 80215-901, Brazil
[6]VALORIZA, Research Centre for Endogenous Resource Valorization, Polytechnic Institute of Portalegre (IPP), 7300-110 Portalegre, Portugal
[7]COPELABS, Universidade Lusófona de Humanidades e Tecnologias, 1749-024 Lisboa, Portugal
[8]Expert Systems and Applications Laboratory (ESALAB), Faculty of Science, University of Salamanca, 37008 Salamanca, Spain
[9]Graduate Program in Applied Computer Science, University of Vale do Itajaí (UNIVALI), Itajaí 88302-202, Brazil

Corresponding author: Stéfano Frizzo Stefenon (stefano.stefenon@udesc.br)

This work was supported in part by the Fundação para a Ciência e a Tecnologia under Project UIDB/04111/2020.

ABSTRACT Contaminated insulators can have higher surface conductivity, which can result in irreversible failures in the electrical power system. In this paper, the ultrasound equipment is used to assist in the prediction of failure identification in porcelain insulators of the 13.8 kV, 60 Hz pin profile. To perform the laboratory analysis, insulators from a problematic branch are removed after an inspection of the electrical system and are evaluated in the laboratory under controlled conditions. To perform the time series predictions, the stacking ensemble learning model is applied with the wavelet transform for signal filtering and noise reduction. For a complete analysis of the model, variations in its configuration were evaluated. The results of root mean square error (RMSE), mean absolute percentage error (MAPE), mean absolute error (MAE), and coefficient of determination (R^2) are presented. To validate the result, a benchmarking is presented with well-established models, such as an adaptive neuro-fuzzy inference system (ANFIS) and long-term short-term memory (LSTM).

INDEX TERMS Electric power system, ensemble learning model, grid inspection, wavelet packet transform.

I. INTRODUCTION

Current electrical demands are growing and it is getting harder to keep the electrical system running, a possible solution to better meet these demands would be to increase the quality in the evaluation of the electrical power system [1]. To maintain transmission and distribution systems working satisfactorily it is necessary to have accurate and comprehensive information on the service performance of the insulators. Over time the insulators may present failures due to several reasons, the more common ones being contamination, cracks caused by vandalism, the nest of birds, and accumulation of dust [2].

The associate editor coordinating the review of this manuscript and approving it for publication was Arpan Kumar Pradhan.

The use of artificial intelligence to predict adverse conditions in the electrical system is a promising alternative to the problem in question, as it can improve the quality of electricity, reducing possible failures. Some researches are focused on load forecasting in electrical systems [3], fault prediction applications in the electrical grid are rarer [4]. According to Santos and Barros [5] a stochastic approach can be used to predict the amplitude and duration of voltage sags when planning the electrical network. This analysis needs to be performed as a network planning criterion, considering the stochastic nature of the energy system failures.

In [6] the problem of power failure is analyzed considering the influence of severe weather, the infrastructure of the electricity grid, and nearby vegetation. Large storms can cause power outages, and forecasting these events can help

This work is licensed under a Creative Commons Attribution 4.0 License. For more information, see https://creativecommons.org/licenses/by/4.0/

maintenance teams prepare for a storm, and thus, take more organized action depending on what might happen. In this way, an interruption prediction model can be used to prevent failures and improve electrical reliability.

To improve security on these networks, it is possible to monitor high voltage circuit breakers (HVCB), to keep the power system stable. Failure recognition can be used to categorize the failure data to identify the type of failure that is occurring. The method proposed by [7], using the support vector machine, achieved promising diagnostics of typical HVCB failures.

Specifically for the prediction of time series for the identification of faults in insulators, Stefenon *et al.* [8] presented the application of adaptive neuro-fuzzy inference system to assess predictability, emitted by an ultrasound device. The study shows that hybrid algorithms in this application outperformed classic algorithms. For the extraction of characteristics, the wavelet transform showed promising results, reducing the forecast error considerably [9].

Through statistical simulations to evaluate the influence of the inherent random errors of the electricity distribution system, it is possible to locate faults using a modern network measurement and monitoring system [10]. Fault location in insulators can be carried out even through aerial inspection. According to [11], the experimentally assessed accuracy can reach 93.69 %. For a good assertiveness in the analysis of ultrasonic signals, in addition to choosing the appropriate model, a complete evaluation of the network configuration is necessary. An artificial neural network that performs well for one type of problem may not be suitable for another.

Applied to the power quality of the electric power grid, [12] performed the location of faults in transmission lines using the ensemble Kalman filter. The algorithm enables accurate identification of faults in transmission lines, minimizing downtime, labor, and costs. Wang *et al.* [13] had promising results applying algorithms that combine complete ensemble empirical mode decomposition with adaptive noise for ground fault detection in a distribution network.

Based on the promising applications of the wavelet transform for feature extraction, as well as the ensemble learning model for time series forecasting, this paper aims to evaluate the forecasting effectiveness of a hybrid wavelet stacking ensemble learning model for ultrasonic signal detection from a contaminated insulator, which may develop a failure over time.

The contributions of this paper for electric power systems research are summarized in the following:

- The first contribution is about the use of ultrasound equipment to identify and prevent failures in the electrical system, which is specific equipment for conducting network inspection. In this paper, we show that the processing of this signal through a hybrid artificial intelligence model can assist the operator in making decisions regarding the maintenance of the system.
- The second contribution is related to the use of the Wavelet transform for filtering and reducing signal noise. The results presented in this paper show that the use of this technique is promising when combined with advanced time series forecasting models.
- The third contribution is related to the use of the stacking ensemble model, which has superior results in accuracy and error reduction than well-established models such as Adaptive Neuro-Fuzzy Inference System (ANFIS) and Long-term Short-Term Memory (LSTM).

The remainder of the paper is organized as follows: In Section II the contaminated insulator problem is presented and the laboratory configuration is detailed. In Section III, the proposed method for evaluating the signal obtained through laboratory tests is conducted. In Section IV, the results obtained are investigated and discussed. Finally, the conclusions are provided in Section V, regarding the applicability of the technique.

II. EVALUATION OF INSULATORS CONTAMINATION

Insulators of Brazil's medium voltage overhead distribution networks are typically built outdoors and are thus exposed to environmental variations [14]. Contamination in insulators does not represent a failure in the system, however, the high concentration of contaminants can increase surface conductivity and impair the insulation of these components, for this reason, this condition needs to be monitored [15]–[17].

Researchers have evaluated the influence of contaminants on the surface of insulating materials. The presence of salt on insulators is the focus of several studies, there are specific analyzes to determine which concentration of salinity generates a problem in these components [18]. In rural regions, there is greater contamination by dust from unpaved streets in addition to organic residues present in these environments. Over time, the contamination that accumulates on the surface of insulators can become encrusted and the rain is not sufficient to clean these insulators [19].

In Figure 1, insulators with different types of contamination can be seen that are found in the field during inspections of the electrical system. The insulator shown in Figure 1A has an accumulation of dust because is installed close to unpaved streets. With a higher level of contamination, fungi can settle on the surface of the insulator, as can be seen in Figure 1B. Over time, contamination becomes strongly stuck to the surface, and thus it is difficult to remove, as can be seen in Figure 1C.

The insulator in Figure 1D has a high level of saline concentration, as it is installed close to the coastal region, however, this contamination is difficult to be perceived with the naked eye. Insulators with saline contamination were not considered in this paper, since the equipment's removed from the problematic branch were in the mountain region.

A. FIELD INSPECTION

Initially, an inspection of the distribution system was carried out in the Riu Rufino city, which is located in the Santa Catarina plateau, in southern, Brazil. In this inspection, possibly

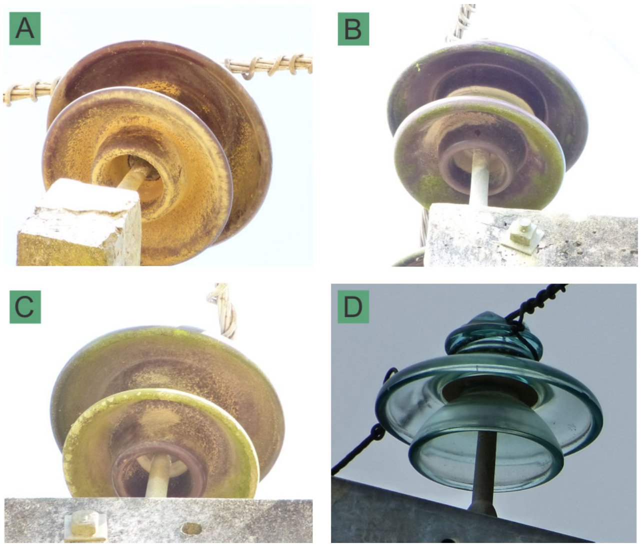

FIGURE 1. **Field contaminated insulators: A) Dust contamination; B) Fungi contamination; C) Contamination strongly stuck; D) Saline contamination.**

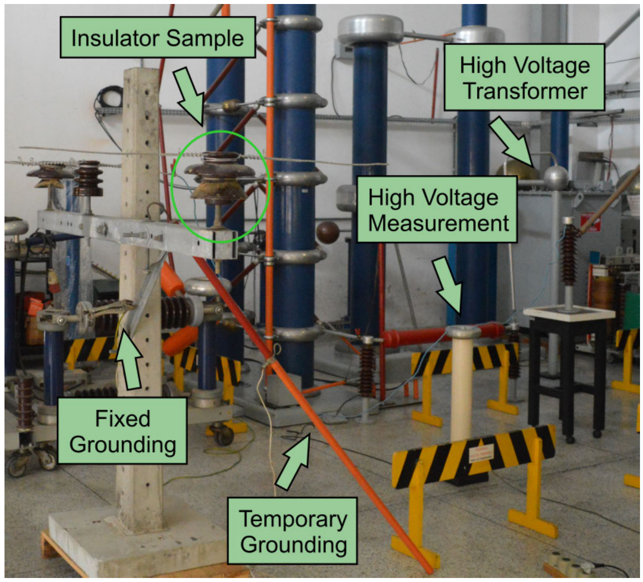

FIGURE 2. **Laboratory analysis setup.**

damaged insulators were reported to the electric utility. The electricity utility removed the components that had an indication of failure in their vicinity, and so these were taken to the laboratory for analysis under controlled conditions.

Field inspections are performed to assess which components are most likely to develop irreversible failures [20]. These inspections are carried out with specific techniques, such as thermovision, radio interference, ultraviolet image, and ultrasound. Equipment that assesses the condition of insulators in the system based on the image can be harmed by interference from solar radiation. Equipment that uses sound can suffer interference from electric motors and other equipment that are close to the systems. In this way, the inspection of the electrical power system is a difficult task to be carried out, which requires specific equipment and specialized technicians [21].

The equipment that has been successfully used for the inspection of electrical power systems is the ultrasound detector, as it is directional and can be adjusted according to the condition to be analyzed. Damaged components can generate ultrasonic noise, which can be captured in a directional way, thus facilitating the exact identification of the source of the possible failure [22]. As ultrasound equipment generates an audible noise that is based on a time series, the evaluation of its continuity in contaminated insulators can facilitate the prediction of the development of a failure. Contaminated insulators do not represent components that must be replaced; however, the permanence of surface contamination can increase partial discharges and leakage current, thus generating irreversible failures [23].

The ultrasound equipment has wide application for the inspection of the electrical power system, however, there is a presence of high-frequency noise in the signal, which is not interesting for analysis since the equipment generates an audible signal. To improve signal forecasting, the wavelet transform is applied in this paper [24].

The application of Wavelet transform for feature extraction coupled with ensemble learning is promising for the diagnosis of failures. According to [25], these techniques can be applied for the investigation of vibration features of motor bearing faults. Also applied to fault diagnosis in rotating machinery based on vibration signals, [26] presents promising results using the combination of these techniques. The results show that the support vector machine (SVM) ensemble can reliably separate different fault conditions and identify the severity of faults, and have a better performance rating than the single SVM.

B. LABORATORY SETUP

The analyzed insulator was assembled in the laboratory without changing the installation pattern used by the energy utility *Centrais Elétricas de Santa Catarina* (CELESC). The insulator was mounted on a 2 m crosshead, the cable was fixed on the insulator using the electric utility's mooring pattern. This assembly is shown in Figure 4. Fixed grounding was used as a reference for high voltage and temporary grounding was used between the measurements for the safety of laboratory operators.

A voltage of 13.8 kV, 60 Hz was applied on the cable, which is the same used in the grid where the insulator was installed previously. The Radar Engineers® (model 250) ultrasound detector was used, to capture the ultrasonic signal from the insulator. The signal was recorded by a computer through its audio connection.

The insulators evaluated in this paper were removed from the field after an inspection of the electrical power system. The local electricity utility requested a specialized team to inspect the network, considering that in adverse weather conditions there was a power shortage at the branch, where the insulators were installed.

The insulators were removed from the field to preserve their original characteristics, for this reason, they were not washed or cleaned for carrying out the experiments. These insulators were installed on a rural branch that is close to the unpaved street, thus, the insulators had an accumulation of dust and organic residues encrusted (strongly attached) under their surface.

C. RAW SIGNAL

The ultrasound equipment pre-processes the signal and generates an audible response for the operator. This signal is evaluated by the operator to identify possible failures in the electrical system. During the experiment, the signal was recorded with a sampling rate of 48 kHz, which corresponds to a recorded point every 20.83 μs. As ultrasonic noise is based on a time series that can vary depending on the condition of the insulator, the forecasting of the ultrasonic noise variation may indicate the presence of discharges that may be related to insulation failure.

Considering an audible signal, frequencies higher than 20 kHz are not considered in this research and the analyzed signal has 20,000 samples. From these samples, using the Holdout approach, the data set was divided for training and testing the network. The analyses were performed considering an Intel Core I5-7400, 20 GB of Random-Access Memory, with GeForce GTX 1050TI NVIDIA video card, the Matlab software was used.

III. HYBRID ENSEMBLE STACKING

In this section the proposed method is detailed. The proposed framework is a hybrid approach composed of wavelet packet transform, employed to signal denoising, and a stacking ensemble learning for insulators contamination forecasting from the distribution network.

The ensemble learning approach is a promising technique for diagnosing failures [27]. It is an approach employed in classification, time series forecasting [28], and nonlinear system identification problems to obtain an accurate model [29]. This methodology is based on the dived-to-conquer framework, in which, several base-learners (weak) are combined (by average rule for regression problems) with the purpose of building an efficient model [30]. Applying this technique, it is possible to evaluate large data sets to increase defective minority classes [31].

A. WAVELET PACKET TRANSFORM

A wavelet is a waveform of effectively limited duration that has a null average value. It is a multi-resolution signal analysis method widely used to deal with non-linear and non-stationary time series [32]. While the Fourier transform describes a signal as a sum-up of sines and cosines, the wavelet transform expands the original signal into a set (coefficient wavelets) of shifted and scaled versions of the base wavelet, named mother wavelet, it can represent the data in the time domain and frequency [33].

To perform wavelet analysis, continuous wavelet transform (CWT) and discrete wavelet transform (DWT) versions should be used. Whereas the CWT has a considerable amount of wavelet coefficients as result, DWT operates on scales with discrete numbers, and a subset of scales and positions are adopted, named dyadic scales and positions. Despite DWT is an effective tool for signal decomposition and feature extraction, it has two main drawbacks, the sample size of the signal should be kind of 2^J, in which J is the wavelet decomposition level, and the circular shift of the series has different empirical power spectra. In this respect, an improved version of DWT can be considered, such as wavelet packet transform (WPT) [34].

The WPT is attractive once can generating more frequency bands and enhancing the extraction of relevant information from the original signal. As well as DWT, the WPT has been successfully applied to solve several engineering problems. The WPT decomposes each iteration and extracts a coefficient, so the number of coefficients depends on how many iterations were performed. The decomposition of the wavelet obtains several levels of packets nodes, from the wavelet packet (WP) a tree structure is formed dividing the approximation of the coefficients [35]. The process of decomposition and reconstruction of the signal through the wavelet packets is shown in Figure 3.

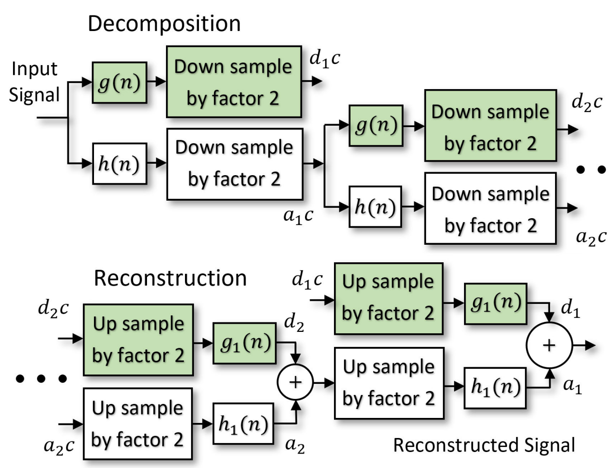

FIGURE 3. Decomposition and reconstruction of wavelet packets.

To have the best performance in the algorithm, an optimized tree is used. Each WP coefficient is specific with a frequency resolution level associated with a scale parameter l and an oscillation parameter n. While wavelet transform decomposes only low-frequency components, WPT decomposes all components at all levels and nodes. Concepts such as entropy, energy, and variation are used to calculate WP coefficients. From the WPT the wavelet energy coefficient (WEC) is obtained and applied in the time series, as the concepts of entropy, energy, and variation are used, the resulting signal loses less information than other techniques [36].

B. STACKED GENERALIZATION

The stacked generalized is an ensemble learning model based on the principle of dived-to-conquer [37], which improves models' accuracy by integrating models through layers that have been successfully applied to solve problems in several fields of knowledge. Usually, two layers are commonly adopted, however, it may not be limited to that. In fact, in the first layer (layer-0), base-learners (weak-learner, or weak-models) are trained and its predictions are used in the next layer. In the sequence, for layer-1 a meta-learner (strong-learner, or strong-model) is trained, whose predictions of the previous layer are adopted as system inputs and predictions are obtained.

The effectiveness of this methodology and the main advantage lies in the fact that different models can produce different predictions, and the meta-learner acquires knowledge with these results [38]. This approach reaches the improvement of forecasting output due to possible variance reduction of forecast error or correction of biases. Results from this learning process tend to converge for an improved solution when compared to the base-learners. Alongside this, a disadvantage of this approach is associated with the choice of the number of base-learners employed. However, with the adoption of general-purpose machine learning wrappers freely available, this may be overcome by testing many different base-learners as the syntax is unified.

In this paper, the base and meta-learners are based on support vector regression (SVR), which is trained based on a set of inputs to predict an output [39]. The SVR is chosen because it has as its main advantage its capacity to capture the predictor nonlinearity and then use it to improve the insulator's contamination forecasting from the distribution network. Let $[x_i, y_i]$ an ordered pair of observations, in which $x_i \in R^d$ is a set of input variables, and $y_i \in R$ its respective output variable. The main concept behind the SVR is to map low-dimensional input data into high-dimensional space based on the non-linear mapping or kernel functions.

To create the proposed ensemble, some different kernel functions $\mathrm{K}(x_j,x_k)$, equivalent to an inner product between observations (x_j,x_k) in some feature space, are combined. In fact, they are Gaussian (1), Linear (2), and Polynomial (3) functions, which are stated as follows,

$$\mathrm{K}(x_j, x_k) = exp(-\left\|x_j - x_k\right\|^2), \tag{1}$$

$$\mathrm{K}(x_j, x_k) = x_{j'} x_k, \tag{2}$$

$$\mathrm{K}(x_j, x_k) = \left(1 + x_{j'} x_k\right)^q. \tag{3}$$

Figure 4 illustrates the proposed stacking ensemble model for insulators contamination prediction, the model uses the result of applying the WEC as an input signal. The procedure of the Wavelet transform for the extraction of features and noise reduction is presented in detail in Figure 3.

The main criteria adopted to evaluate the proposed model according to the global error, are root mean square error (RMSE), mean absolute percentage error (MAPE), mean absolute error (MAE), and coefficient of determination R^2 [40]. While the criteria RMSE, MAE, and MAE compute the performance of models regarding the errors, which a lower value is desirable, the R^2 criterion shows the variability explained by the model, where a high value is need [41].

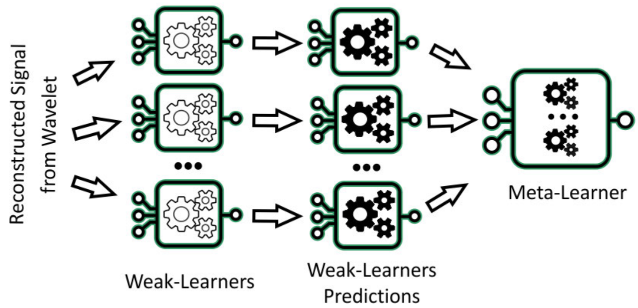

FIGURE 4. Stacking Ensemble model.

Additionally, the above-described performance measures, based on the best configuration found for the proposed model, the statistical performance of the algorithm in relation to 50 analyzes will be evaluated. In fact, the variance (VAR), covariance (COV), mean, and standard deviation (Std. D) indicators are presented. For the final performance test of the model, the Wilcoxon Signed Rank Test is presented and discussed [42].

C. BENCHMARKING

For comparative analysis with the proposed method, LSTM and ANFIS were used. Variations in these models were made for a complete assessment. The LSTM is a recurrent neural network architecture, used in the field of deep learning. The LSTM can process entire strings of data and for this reason, it is well applied for chaotic time series and anomaly detection [43]. For a complete analysis of LSTM, 3 optimizers were used, being: stochastic gradient descent with momentum (SGDM), root mean square propagation (RMSProp), and adaptive moment estimation (ADAM).

The stochastic gradient descent algorithm can oscillate along the steepest descent path towards the optimum, to solve this, a moment term is added to the parameter update to reduce this oscillation [44]. The LSTM with the SGDM optimizer is a promising algorithm and will be compared in this paper [45].

The RMSProp uses the learning rates that differ by parameter and can automatically adapt to the loss function being optimized. Thus, the algorithm maintains a moving average of the element-wise squares of the parameter gradients. The ADAM optimization method calculates adaptive learning rates for each parameter [46].

The structure of the ANFIS is a combination of a fuzzy inference system and a neural network, some methods of cluster organization can be used for this model. Considering a Subtractive Clustering Structure (SCS), which requires a separate dataset and different arguments, it is possible to extract the sets of rules that can identify the behavior of the time series [47].

The Fuzzy C-Means (FCM) inference system automatically selects the number of clusters and randomly distributes the coefficients for each sample in the dataset. The FCM repeats this procedure until it reaches convergence, which means that each cluster must be calculated considering its membership level [48].

A summary of the entire procedure performed for this paper is presented in Figure 5, the project was separated into 3 stages. The first stage was carried out through a research project with the local electric utility.

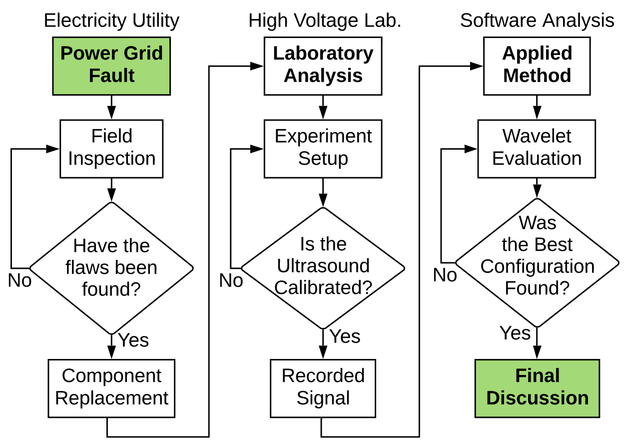

FIGURE 5. Project flowchart.

In this research project, the locations with reported failures were indicated by the electric utility, and an inspection team conducted a field analysis in these electric power grids. After the identification of failures, the components were removed and replaced by the electric utility.

In the second stage, the defective components were taken to the high voltage laboratory where they were tested under controlled conditions. These components were evaluated, and the signal was recorded. The last stage is the evaluation of the proposed method to the signal recorded of the contaminated insulator that the focus of this paper.

For a complete assessment of the model, some configuration parameters were evaluated, the first parameter evaluated was the size of the data set for training and testing the network, then the kernel function (as base-leaner) was evaluated, we evaluated the use of Wavelet to extract the feature and noise reduction, finally, with the best configuration found, a statistical analysis was performed.

IV. ANALYSIS OF APPLIED METHOD

In this section, the evaluation results of the proposed algorithm will be presented. Initially, an analysis of the consequences of possible variations of the model with raw data will be carried out; then the analysis will be presented applying the Wavelet transform to extract characteristics. Subsequently, statistical analysis to the configuration for the best model and a comparative benchmarking is performed.

A. PARAMETER CHANGE ASSESSMENT

The first comparative analysis assesses the size of the division of training dataset in relation to the test, considering the holdout approach. In this respect, the training (Train) data is not used for network testing (Test). In fact, Table 1 illustrates the results for a stacking ensemble, in which the base-learner is the SVR with linear kernel, while the meta-leaner is the SVR with Gaussian kernel.

TABLE 1. Training and testing size evaluation.

Train – Test	RMSE	MAPE	MAE	R^2
90 – 10	**0.0500**	0.4987	3.08×10^{-4}	0.2056
80 – 20	0.0506	0.4340	1.13×10^{-3}	0.1976
70 – 30	0.0502	**0.0229**	7.11×10^{-4}	**0.2160**
60 – 40	0.0503	0.1803	3.58×10^{-4}	0.2110
50 – 50	0.0502	0.1013	4.53×10^{-4}	0.2052
40 – 60	0.0501	43.464	6.79×10^{-4}	0.1979
30 – 70	0.0502	21.091	6.63×10^{-4}	0.2132
20 – 80	0.0507	0.0629	1.38×10^{-3}	0.1953
10 – 90	0.0508	0.4480	$\mathbf{1.59}\times10^{-4}$	0.1816

In this preliminary assessment, it can be seen that the values of R^2 are low for all combinations of datasets. The best results from MAPE and R^2 were found using 70 % of the data for training and 30 % of the data for testing, so this configuration was used for the following analyzes. There was little variation in the RMSE, with the maximum difference in this metric being only 1.6 %.

Table 2 shows the performance for some stacking ensemble structures, according to the setting defined in Table 1. The variation in the kernel functions did not generate major differences in terms of RMSE. The use of more than 2 layers made the algorithm considerably slower for convergence and did not represent significant improvements in the forecast, therefore, these results are not considered.

TABLE 2. Performance measures for different structures.

Base-Learner – Meta-Learner	RMSE	MAPE	MAE	R^2
LINE – GAUS	0.0502	**0.0229**	$\mathbf{1.11}\times10^{-4}$	0.2160
LINE – POLY	0.0502	11.103	1.54×10^{-4}	0.2084
GAUS – LINE	0.0499	0.4169	1.27×10^{-3}	0.2035
GAUS – GAUS	0.0501	23.420	1.82×10^{-3}	0.1902
GAUS – POLY	0.0500	0.5737	5.81×10^{-4}	0.1844
POLY – POLY	0.0498	32.808	6.79×10^{-4}	**0.2178**
POLY – GAUS	**0.0497**	26.533	6.27×10^{-3}	0.2172
POLY – LINE	0.0505	23.135	4.59×10^{-4}	0.2071

Using the SVR with Polynomial (POLY) kernel as base-learner, in general, allowed to achieve good results regarding RMSE and R^2. However the MAPE and MAE values were among the worst results in these comparison. The use of 2-layers with the linear (LINE) kernel function (as base-leaner) and Gaussian (GAUS) kernel function (as meta-learner) generated the best result in the calculation of MAPE and MAE. Furthermore, this configuration had a satisfactory RMSE and R^2 result, so this configuration was defined as the standard model stacking ensemble.

B. WAVELET ENSEMBLE LEARNING RESULTS

The use of correct WPT structure allows achieving better accuracy in respect of forecasting, once that to consider an inadequate configuration can result in loss of the signal characteristic. Moreover, The variation in the number of nodes results in a significant change in the WEC response. In fact, Table 3 presents the results for the hybrid proposed model, which considers a stacking ensemble with Linear and Gaussian kernels, in layers-0 and 1, for different WPT settings.

TABLE 3. Results of applying WEC in different configurations.

Levels	Nodes	RMSE	MAPE	MAE	R^2
3	1	0.0187	0.1411	3.33×10^{-3}	0.8660
	3	0.0066	0.0719	2.94×10^{-4}	0.9797
	7	**0.0019**	0.0300	1.40×10^{-3}	**0.9982**
4	1	0.0193	0.1414	3.40×10^{-3}	0.8559
	3	0.0065	0.0758	3.09×10^{-4}	0.9809
	7	**0.0019**	0.2610	3.23×10^{-4}	0.9981
5	1	0.0197	0.0903	3.38×10^{-3}	0.8480
	3	0.0064	0.1329	8.58×10^{-4}	0.9808
	7	**0.0019**	0.2729	$\mathbf{1.90}\times10^{-4}$	0.9981
6	1	0.0190	0.9525	3.39×10^{-4}	0.8606
	3	0.0068	0.2027	4.46×10^{-4}	0.9780
	7	**0.0019**	**0.0210**	5.50×10^{-4}	0.9980

The best configurations of the WPT were found with 1, 3, and 7 nodes. Using 2, 4, 5, 6, or more than 7 nodes, there was a loss of characteristics, so these values were discarded. The variation of levels in the Wavelet transform did not result in visually perceptible changes in the WEC response. The best predictability result was obtained using 7 nodes, with considerably lower RMSE, and with higher R^2.

Considering that RMSE is a measure of error and R^2 is a measure of accuracy, the lower the RMSE and the higher the R^2 is a better result in this assessment. Changing the number of levels did not generate such representative variations in these parameters. The best MAPE was obtained with 6 levels and the best MAE was obtained with 5 levels. The application of the WPT with 7 nodes, for the considered signal, can be viewed in Figure 6, for a better view, it's presented in a window of 1,000 samples.

According to results of Table 3, considering the presented performance criteria, the WPT composed of 3 levels and 7 nodes configuration was the one that presented the best result and, therefore, the statistical analysis for the global evaluation of the algorithm will be performed with this configuration. Using this configuration, coupled with stacking ensemble which considers linear and Gaussian kernels, as base and meta-learners, respectively, the forecast result compared to the observed signal is shown in Figure 7.

All changes in the levels were considered, with the exception of values less than 3 and greater than 6. Due to the variation in the number of nodes, it is necessary to have at least 3 levels for the algorithm to compute the transform and values greater than 6 do not represent major changes, so they are disregarded. As can be seen in Table 3, the application of the Wavelet transform through the WEC generated considerably superior results in terms of reducing error and improving accuracy. This fact confirms that the hybrid algorithm is superior to the application of classical techniques to the problem under analysis.

The application of the Wavelet transform proved to be an excellent alternative to be used with the Ensemble Stacking for signal forecasting [8]. As presented in these results, the WEC must be tested in its variations, considering that an improper configuration can result in loss of signal characteristics.

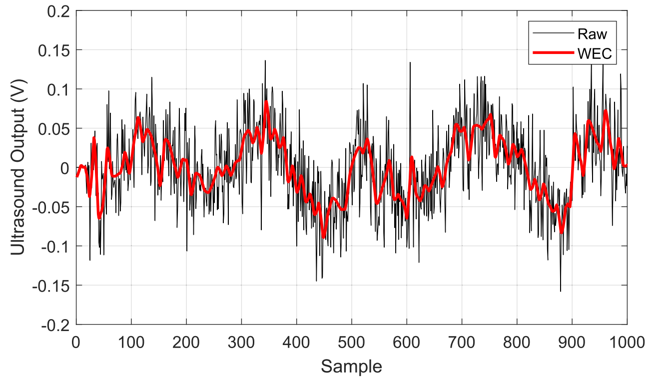

FIGURE 6. Wavelet energy coefficient applied to the raw signal.

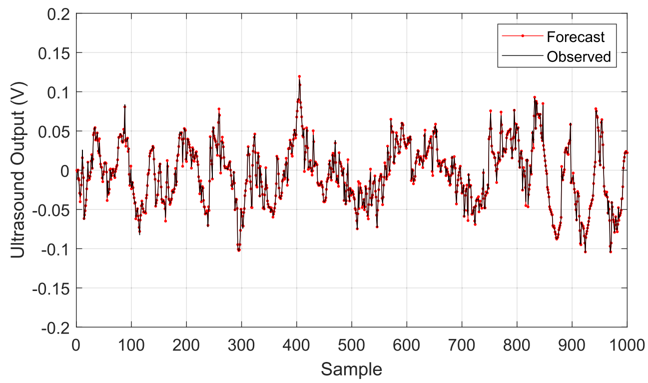

FIGURE 7. Raw signal of contaminated insulator.

C. BENCHMARKING RESULTS

Using the ADAM optimizer, the best results were obtained for RMSE, MAE, and R^2, as can be seen in Table 4. The LSTM had the best accuracy of 55.52 %, which is lower than the average result of 99.80 % presented in Table 6 for the proposed algorithm. The variation in the number of hidden units did not represent an improvement that overcomes the Hybrid Wavelet Ensemble Stacking. To standardize the analyzes, the hyperbolic tangent activation function was used, which is suitable for LSTM [43]. The use of 10 hidden units resulted in lower accuracy results for all optimizers.

TABLE 4. Long short-term memory results.

Optimizer	Hidden Units	RMSE	MAPE	MAE	R^2
SGDM	10	0.0394	22.049	1.04×10^{-3}	0.3991
	50	0.0395	0.5545	1.19×10^{-3}	0.3979
	100	0.0394	30.161	9.65×10^{-4}	0.3983
	150	0.0394	0.4614	9.55×10^{-4}	0.3982
	200	0.0395	0.4747	1.66×10^{-3}	0.3977
ADAM	10	0.0391	16.332	$\mathbf{1.02}\times10^{-4}$	0.4078
	50	0.0341	80.944	4.42×10^{-3}	0.5507
	100	**0.0334**	0.5761	1.64×10^{-3}	**0.5679**
	150	0.0363	1.3863	4.09×10^{-4}	0.5316
	200	0.0345	1.0034	1.32×10^{-4}	0.5386
RMSProp	10	0.0394	0.9172	1.41×10^{-3}	0.3997
	50	0.0345	18.089	5.97×10^{-3}	0.5399
	100	0.0352	**0.4452**	1.22×10^{-3}	0.5198
	150	0.0350	0.5203	1.23×10^{-3}	0.5255
	200	0.0410	2.2993	3.14×10^{-3}	0.4491

The results for the error assessment metrics were also worse than Hybrid Wavelet Ensemble Stacking, with the RMSE being 0.0341 compared to 0.0019. The best MAE obtained with the LSTM was 1.0219×10^{-4} and the best MAPE was 0.4452, which are also inferior to the proposed method. The SGDM and RMSProp optimizers were inferior to the ADAM optimizer in all RMSE and R^2 results.

The size of the dataset used for this analysis was the same as the other methods evaluated, in which 70 % of the data for training and 30 % of the data for the test were standardized. In the SCS and FCM, each output variable has one output membership function for each fuzzy cluster. For comparison purposes, all the clustering outputs types were Sugeno system types.

Possible configurations in the models have been tested and are presented in Table 5. For SCS, the Influence Radius (IR) was varied, the network did not converge to values less than 0.2 and greater than 0.5. In FCM the variation was made in the number of clusters, and with 1 cluster the network does not converge and with more than 14 clusters there is no improvement in results.

TABLE 5. Adaptive neuro-fuzzy inference system results.

Structure	Output Mem. Func.	RMSE	MAPE	MAE	R^2
SCS	0.20 IR	0.0373	7.2909	2.55×10^{-4}	0.4621
	0.25 IR	**0.0372**	1.8310	2.19×10^{-4}	0.4646
	0.30 IR	**0.0372**	0.6127	2.16×10^{-4}	0.4642
	0.35 IR	**0.0372**	8.6728	2.02×10^{-4}	0.4643
	0.40 IR	**0.0372**	30.185	2.33×10^{-4}	0.4645
	0.45 IR	**0.0372**	2.4821	2.16×10^{-4}	0.4645
	0.50 IR	**0.0372**	1.0812	2.21×10^{-4}	0.4647
FCM	2 Clusters	**0.0372**	0.0579	2.23×10^{-4}	**0.4653**
	4 Clusters	0.0373	0.0476	2.32×10^{-4}	0.4625
	6 Clusters	0.0374	**0.0430**	2.35×10^{-4}	0.4600
	8 Clusters	0.0375	0.3599	2.02×10^{-4}	0.4567
	10 Clusters	0.0375	0.3497	2.08×10^{-4}	0.4552
	12 Clusters	0.0375	3.5001	$\mathbf{1.16}\times10^{-4}$	0.4571
	14 Clusters	0.0377	1.8815	1.88×10^{-4}	0.4508

Despite resulting higher RMSE values than LSTM, ANFIS was more stable, with little variation in this measure. The best value of R^2 for ANFIS was also lower than the result of the LSTM. Comparing to the Hybrid Wavelet Stacking Ensemble proposed in this paper, both techniques were inferior to the accuracy and error values.

The only result that was superior to the proposed method was the MAPE using some FCM configurations for the ANFIS model, however, it is not possible to state that this value has a great influence on the analysis, since there is great variation in the MAPE results for this benchmarking. Furthermore, the most important metrics for time series analysis are RMSE and R^2, which were superior using the proposed method in this paper.

D. STATISTICAL EVALUATION

Statistical analysis is used to assess the robustness of the algorithm, when the algorithm is suitable for the problem, there should be no great variability in the statistical results. In fact for the proposed wavelet stacking ensemble, this assessment is shown in Table 6, for 50 independent runs.

TABLE 6. Hybrid wavelet stacking ensemble statistical results.

Param.	RMSE	MAPE	MAE	R^2
Mean	0.0019	0.0857	8.02×10^{-5}	0.9980
VAR	1.6×10^{-9}	1.6×10^{-2}	3.8×10^{-9}	7.3×10^{-9}
Std. D	4.0×10^{-5}	1.3×10^{-1}	6.2×10^{-15}	8.6×10^{-5}
COV	7.2×10^{-11}	2.4×10^{-3}	1.1×10^{-10}	5.3×10^{-10}

The variance in RMSE, MAE, and R^2 is low, only MAPE has a bigger variance of the resulting values, this also occurs with standard deviation and with covariance. Considering that the main metrics used in the literature to evaluate the time series are RMSE and R^2 [49], it can be said that there is little variability in the results showing that the proposed algorithm is stable.

For a comparative analysis in relation to variation of the algorithm, we present in Table 7 a statistical evaluation of the ANFIS model and in Table 8 of the LSTM model, both from the best configuration found for the models in question.

TABLE 7. ANFIS statistical results.

Param.	RMSE	MAPE	MAE	R^2
Mean	0.0372	3.8361	2.2×10^{-4}	0.4653
VAR	2.4×10^{-11}	4.3×10^{2}	2.1×10^{-10}	1.9×10^{-8}
Std. D	4.9×10^{-6}	2.1×10^{1}	1.4×10^{-5}	1.4×10^{-4}
COV	4.2×10^{-13}	4.4184	5.1×10^{-12}	3.5×10^{-10}

As can be seen, despite the low variance in the ANFIS results, this model presents considerably less accuracy when compared to the proposed method. The same statement can be made in relation to the LSTM model, which shows to be robust with low variance, however with greater error and less accuracy than the proposed model. Comparatively, the LSTM model had better results than the ANFIS model in the statistical analysis, having a higher accuracy average and lower variance values for accuracy.

According to the non-parametric Friedman test, the forecasting models achieved errors statistically different for MAE

TABLE 8. LSTM statistical results.

Param.	RMSE	MAPE	MAE	R^2
Mean	0.0372	3.8361	2.2×10^{-4}	0.4653
VAR	2.4×10^{-11}	4.3×10^{2}	2.1×10^{-10}	1.9×10^{-8}
Std. D	4.9×10^{-6}	2.1×10^{1}	1.4×10^{-5}	1.4×10^{-4}
COV	4.2×10^{-13}	4.4184	5.1×10^{-12}	3.5×10^{-10}

TABLE 9. Wilcoxon signed rank test.

Criteria	Comparison	p-value	Is significant the difference?
MAE	ANFIS vs LSTM	3.2×10^{-5}	Yes
	ANFIS vs Ensemble	7.8×10^{-6}	Yes
	Ensemble vs LSTM	3.8×10^{-14}	Yes
MAPE	ANFIS vs LSTM	3.2×10^{-9}	Yes
	ANFIS vs Ensemble	0.76	No
	Ensemble vs LSTM	3.1×10^{-11}	Yes
R^2	ANFIS vs LSTM	3.1×10^{-14}	Yes
	ANFIS vs Ensemble	1.3×10^{-5}	Yes
	Ensemble vs LSTM	6.0×10^{-7}	Yes
RMSE	ANFIS vs LSTM	3.1×10^{-14}	Yes
	ANFIS vs Ensemble	1.3×10^{-5}	Yes
	Ensemble vs LSTM	6.0×10^{-7}	Yes

(chi-squared = 82.84, df = 2, p-value < 2.2e-16), MAPE (chi-squared = 55.96, df = 2, p-value = 7.054e-13), R^2 (chi-squared = 96.16, df = 2, p-value < 2.2e-16), and RMSE (chi-squared = 96.16, df = 2, p-value < 2.2e-16). Considering the Wilcoxon signed rank test, the Ensemble approach have errors statistically lower than the ANFIS and LSTM. Also, the p-value of comparisons is presented in Table 9.

V. FINAL DISCUSSION

The results of applying the proposed algorithm were promising, considering that it is possible to reach an average determination coefficient of 0.9980. Comparatively, the results of the proposed algorithm are much higher than the application of Ensemble Stacking without using the Wavelet transform, which had a result of only 0.2367. This shows that the hybrid algorithm had a better response than the application of the classic technique.

The application of the proposed technique can become a very promising tool for the evaluation of the electrical system, as, as presented in this work, it is possible to make a prediction with good accuracy of a signal with many nonlinearities. The proposed method can be applied to other applications, not only related to insulators.

The use of the proposed method proved to be better than LSTM and ANFIS in several metrics for the forecasting of time series covered in this paper. For the LSTM, even with the variation in the optimizer and the number of hidden units, the results were lower. The modification in the structure of the ANFIS model also did not result in higher values than the Hybrid Wavelet Stacking Ensemble presented in this paper.

The ultrasonic signal evaluated in this paper can be used for other equipment in the high voltage electrical power networks. Being equipment that has a high capacity to differentiate adverse conditions and prevent failures in the electrical system may result in power outages.

In future works, the proposed method presented in this paper can be extended to other components of the network, in order to analyze the partial discharges that occur in various equipment of the electrical system.

ACKNOWLEDGMENT

The authors would like to thank the Coordination for the Improvement of Higher Education Personnel (CAPES), awarding a doctoral scholarship to one of the authors. This work was supported in part by the Fundação para a Ciência e a Tecnologia under Project UIDB/04111/2020.

REFERENCES

[1] M. H. D. M. Ribeiro, S. F. Stefenon, J. D. de Lima, A. Nied, V. C. Mariani, and L. S. Coelho, "Electricity price forecasting based on self-adaptive decomposition and heterogeneous ensemble learning," *Energies*, vol. 13, no. 19, p. 5190, Oct. 2020, doi: 10.3390/en13195190.

[2] M. P. Corso, S. F. Stefenon, V. F. Couto, S. H. L. Cabral, and A. Nied, "Evaluation of methods for electric field calculation in transmission lines," *IEEE Latin Amer. Trans.*, vol. 16, no. 12, pp. 2970–2976, Dec. 2018, doi: 10.1109/TLA.2018.8804264.

[3] X. Zhang, J. Wang, and K. Zhang, "Short-term electric load forecasting based on singular spectrum analysis and support vector machine optimized by cuckoo search algorithm," *Electr. Power Syst. Res.*, vol. 146, pp. 270–285, May 2017, doi: 10.1016/j.epsr.2017.01.035.

[4] S. Lan, M.-J. Chen, and D.-Y. Chen, "A novel HVDC double-terminal non-synchronous fault location method based on convolutional neural network," *IEEE Trans. Power Del.*, vol. 34, no. 3, pp. 848–857, Jun. 2019, doi: 10.1109/TPWRD.2019.2901594.

[5] A. dos Santos and M. T. C. de Barros, "Voltage sag prediction for network planning," *Electr. Power Syst. Res.*, vol. 140, pp. 976–983, Nov. 2016, doi: 10.1016/j.epsr.2016.03.033.

[6] D. W. Wanik, J. R. Parent, E. N. Anagnostou, and B. M. Hartman, "Using vegetation management and LiDAR-derived tree height data to improve outage predictions for electric utilities," *Electr. Power Syst. Res.*, vol. 146, pp. 236–245, May 2017, doi: 10.1016/j.epsr.2017.01.039.

[7] M. Fei, P. Yi, Z. Kedong, and Z. Jianyong, "On-line hybrid fault diagnosis method for high voltage circuit breaker," *J. Intell. Fuzzy Syst.*, vol. 33, no. 5, pp. 2763–2774, Oct. 2017, doi: 10.3233/JIFS-169325.

[8] S. F. Stefenon, R. Z. Freire, L. dos Santos Coelho, L. H. Meyer, R. B. Grebogi, W. G. Buratto, and A. Nied, "Electrical insulator fault forecasting based on a wavelet neuro-fuzzy system," *Energies*, vol. 13, no. 2, p. 484, Jan. 2020, doi: 10.3390/en13020484.

[9] J. Zhao and C.-M. Lin, "Multidimensional classifier design using wavelet fuzzy brain emotional learning neural networks," *J. Intell. Fuzzy Syst.*, vol. 36, no. 2, pp. 1099–1107, Mar. 2019, doi: 10.3233/JIFS-169884.

[10] P. A. H. Cavalcante and M. C. Almeida, "Fault location approach for distribution systems based on modern monitoring infrastructure," *IET Gener., Transmiss. Distrib.*, vol. 12, no. 1, pp. 94–103, Jan. 2018, doi: 10.1049/iet-gtd.2017.0153.

[11] H. Jiang, X. Qiu, J. Chen, X. Liu, X. Miao, and S. Zhuang, "Insulator fault detection in aerial images based on ensemble learning with multi-level perception," *IEEE Access*, vol. 7, pp. 61797–61810, 2019, doi: 10.1109/ACCESS.2019.2915985.

[12] R. Fan, Y. Liu, R. Huang, R. Diao, and S. Wang, "Precise fault location on transmission lines using ensemble Kalman filter," *IEEE Trans. Power Del.*, vol. 33, no. 6, pp. 3252–3255, Dec. 2018, doi: 10.1109/TPWRD.2018.2849879.

[13] X. Wang, J. Gao, X. Wei, Z. Zeng, Y. Wei, and M. Kheshti, "Single line to ground fault detection in a non-effectively grounded distribution network," *IEEE Trans. Power Del.*, vol. 33, no. 6, pp. 3173–3186, Dec. 2018, doi: 10.1109/TPWRD.2018.2873017.

[14] S. F. Stefenon, J. P. Americo, L. H. Meyer, R. B. Grebogi, and A. Nied, "Analysis of the electric field in porcelain pin-type insulators via finite elements software," *IEEE Latin Amer. Trans.*, vol. 16, no. 10, pp. 2505–2512, Oct. 2018, doi: 10.1109/TLA.2018.8795129.

[15] Y. Liu, B. X. Du, and M. Farzaneh, "Self-normalizing multivariate analysis of polymer insulator leakage current under severe fog conditions," *IEEE Trans. Power Del.*, vol. 32, no. 3, pp. 1279–1286, Jun. 2017, doi: 10.1109/TPWRD.2017.2650214.

[16] B. Cao, L. Wang, and F. Yin, "Measurement of saturated water absorption of the contamination layer deposited on insulator surface," *IEEE Sensors J.*, vol. 19, no. 22, pp. 10804–10811, Nov. 2019, doi: 10.1109/JSEN.2019.2932192.

[17] D. Sadykova, D. Pernebayeva, M. Bagheri, and A. James, "IN-YOLO: Real-time detection of outdoor high voltage insulators using UAV imaging," *IEEE Trans. Power Del.*, vol. 35, no. 3, pp. 1599–1601, Jun. 2020, doi: 10.1109/TPWRD.2019.2944741.

[18] A. K. Abouzeid, A. El-Hag, and K. Assaleh, "Equivalent salt deposit density prediction of silicone rubber insulators under simulated pollution conditions," *Electr. Power Compon. Syst.*, vol. 46, no. 10, pp. 1123–1133, Jun. 2018, doi: 10.1080/15325008.2018.1488303.

[19] Z. Zhang, D. Zhang, J. You, J. Zhao, X. Jiang, and J. Hu, "Study on the DC flashover performance of various types of insulators with fan-shaped nonuniform pollution," *IEEE Trans. Power Del.*, vol. 30, no. 4, pp. 1871–1879, Aug. 2015, doi: 10.1109/TPWRD.2014.2388215.

[20] A. Ibrahim, A. Dalbah, A. Abualsaud, U. Tariq, and A. El-Hag, "Application of machine learning to evaluate insulator surface erosion," *IEEE Trans. Instrum. Meas.*, vol. 69, no. 2, pp. 314–316, Feb. 2020, doi: 10.1109/TIM.2019.2956300.

[21] M. Dong, B. Wang, M. Ren, C. Zhang, W. Zhao, and R. Albarracin, "Joint visualization diagnosis of outdoor insulation status with optical and acoustical detections," *IEEE Trans. Power Del.*, vol. 34, no. 4, pp. 1221–1229, Aug. 2019, doi: 10.1109/TPWRD.2018.2870080.

[22] S. Polisetty, A. El-Hag, and S. Jayram, "Classification of common discharges in outdoor insulation using acoustic signals and artificial neural network," *High Voltage*, vol. 4, no. 4, pp. 333–338, Dec. 2019, doi: 10.1049/hve.2019.0113.

[23] T. V. Ferreira, A. D. Germano, and E. G. da Costa, "Ultrasound and artificial intelligence applied to the pollution estimation in insulations," *IEEE Trans. Power Del.*, vol. 27, no. 2, pp. 583–589, Apr. 2012, doi: 10.1109/TPWRD.2011.2178042.

[24] N. F. S. Neto, S. F. Stefenon, L. H. Meyer, R. Bruns, A. Nied, L. O. Seman, G. V. Gonzalez, V. R. Q. Leithardt, and K.-C. Yow, "A study of multilayer perceptron networks applied to classification of ceramic insulators using ultrasound," *Appl. Sci.*, vol. 11, no. 4, p. 1592, Feb. 2021, doi: 10.3390/app11041592.

[25] W. He, Y. Zi, B. Chen, F. Wu, and Z. He, "Automatic fault feature extraction of mechanical anomaly on induction motor bearing using ensemble super-wavelet transform," *Mech. Syst. Signal Process.*, vols. 54–55, pp. 457–480, Mar. 2015, doi: 10.1016/j.ymssp.2014.09.007.

[26] Q. Hu, Z. He, Z. Zhang, and Y. Zi, "Fault diagnosis of rotating machinery based on improved wavelet package transform and SVMs ensemble," *Mech. Syst. Signal Process.*, vol. 21, no. 2, pp. 688–705, Feb. 2007, doi: 10.1016/j.ymssp.2006.01.007.

[27] Z. Wu, W. Lin, and Y. Ji, "An integrated ensemble learning model for imbalanced fault diagnostics and prognostics," *IEEE Access*, vol. 6, pp. 8394–8402, 2018, doi: 10.1109/ACCESS.2018.2807121.

[28] M. H. D. M. Ribeiro, V. C. Mariani, and L. D. S. Coelho, "Multi-step ahead meningitis case forecasting based on decomposition and multi-objective optimization methods," *J. Biomed. Informat.*, vol. 111, Nov. 2020, Art. no. 103575, doi: 10.1016/j.jbi.2020.103575.

[29] Y. Wang, K. Zhu, M. Sun, and Y. Deng, "An ensemble learning approach for fault diagnosis in self-organizing heterogeneous networks," *IEEE Access*, vol. 7, pp. 125662–125675, 2019, doi: 10.1109/ACCESS.2019.2925566.

[30] M. H. D. M. Ribeiro, V. H. A. Ribeiro, G. Reynoso-Meza, and L. D. S. Coelho, "Multi-objective ensemble model for short-term price forecasting in corn price time series," in *Proc. Int. Joint Conf. Neural Netw. (IJCNN)*, Budapest, Hungary, Jul. 2019, pp. 1–8, doi: 10.1109/IJCNN.2019.8851880.

[31] R. G. da Silva, M. H. D. M. Ribeiro, S. R. Moreno, V. C. Mariani, and L. D. S. Coelho, "A novel decomposition-ensemble learning framework for multi-step ahead wind energy forecasting," *Energy*, vol. 216, Feb. 2021, Art. no. 119174, doi: 10.1016/j.energy.2020.119174.

[32] Y. Deng, S. Lin, L. Fu, K. Liao, L. Liu, Z. He, S. Gao, and Y. Liu, "New criterion of converter transformer differential protection based on wavelet energy entropy," *IEEE Trans. Power Del.*, vol. 34, no. 3, pp. 980–990, Jun. 2019, doi: 10.1109/TPWRD.2019.2893431.

[33] S. F. Stefenon, C. Kasburg, R. Z. Freire, F. C. S. Ferreira, D. W. Bertol, and A. Nied, "Photovoltaic power forecasting using wavelet neuro-fuzzy for active solar trackers," *J. Intell. Fuzzy Syst.*, vol. 40, no. 1, pp. 1083–1096, Jan. 2021, doi: 10.3233/JIFS-201279.

[34] P. A. Karafotis, V. A. Evangelopoulos, and P. S. Georgilakis, "Evaluation of harmonic contribution to unbalance in power systems under non-stationary conditions using wavelet packet transform," *Electr. Power Syst. Res.*, vol. 178, Jan. 2020, Art. no. 106026, doi: 10.1016/j.epsr.2019.106026.

[35] C. Lin, W. Gao, and M.-F. Guo, "Discrete wavelet transform-based triggering method for single-phase earth fault in power distribution systems," *IEEE Trans. Power Del.*, vol. 34, no. 5, pp. 2058–2068, Oct. 2019, doi: 10.1109/TPWRD.2019.2913728.

[36] F. B. Costa and J. Driesen, "Assessment of voltage sag indices based on scaling and wavelet coefficient energy analysis," *IEEE Trans. Power Del.*, vol. 28, no. 1, pp. 336–346, Jan. 2013, doi: 10.1109/TPWRD.2012.2218626.

[37] M. H. D. M. Ribeiro and L. dos Santos Coelho, "Ensemble approach based on bagging, boosting and stacking for short-term prediction in agribusiness time series," *Appl. Soft Comput.*, vol. 86, Jan. 2020, Art. no. 105837, doi: 10.1016/j.asoc.2019.105837.

[38] M. H. D. M. Ribeiro, R. G. da Silva, V. C. Mariani, and L. S. Coelho, "Short-term forecasting COVID-19 cumulative confirmed cases: Perspectives for Brazil," *Chaos, Solitons Fractals*, vol. 135, Jun. 2020, Art. no. 109853, doi: 10.1016/j.chaos.2020.109853.

[39] Z. Tan, J. Zhang, Y. He, Y. Zhang, G. Xiong, and Y. Liu, "Short-term load forecasting based on integration of SVR and stacking," *IEEE Access*, vol. 8, pp. 227719–227728, 2020, doi: 10.1109/ACCESS.2020.3041779.

[40] V. Leithardt, D. Santos, L. Silva, F. Viel, C. Zeferino, and J. Silva, "A solution for dynamic management of user profiles in IoT environments," *IEEE Latin Amer. Trans.*, vol. 18, no. 7, pp. 1193–1199, Jul. 2020, doi: 10.1109/TLA.2020.9099759.

[41] S. F. Stefenon, M. H. D. M. Ribeiro, A. Nied, V. C. Mariani, L. D. S. Coelho, D. F. M. da Rocha, R. B. Grebogi, and A. E. D. B. Ruano, "Wavelet group method of data handling for fault prediction in electrical power insulators," *Int. J. Electr. Power Energy Syst.*, vol. 123, Dec. 2020, Art. no. 106269, doi: 10.1016/j.ijepes.2020.106269.

[42] P. R. R. De Souza, K. J. Matteussi, A. D. S. Veith, B. F. Zanchetta, V. R. Q. Leithardt, A. L. Murciego, E. P. De Freitas, J. C. S. D. Anjos, and C. F. R. Geyer, "Boosting big data streaming applications in clouds with BurstFlow," *IEEE Access*, vol. 8, pp. 219124–219136, 2020, doi: 10.1109/ACCESS.2020.3042739.

[43] C. Kasburg and S. F. Stefenon, "Deep learning for photovoltaic generation forecast in active solar trackers," *IEEE Latin Amer. Trans.*, vol. 17, no. 12, pp. 2013–2019, Dec. 2019, doi: 10.1109/TLA.2019.9011546.

[44] S. F. Stefenon, M. C. Silva, D. W. Bertol, L. H. Meyer, and A. Nied, "Fault diagnosis of insulators from ultrasound detection using neural networks," *J. Intell. Fuzzy Syst.*, vol. 37, no. 5, pp. 6655–6664, Nov. 2019, doi: 10.3233/JIFS-190013.

[45] Y. Guan, Y. Fu, L. Chen, G. Liu, and L. Sun, "Belief-rule-base inference method based on gradient descent with momentum," *IEEE Access*, vol. 9, pp. 34487–34499, 2021, doi: 10.1109/ACCESS.2021.3061679.

[46] S. F. Stefenon, N. W. Branco, A. Nied, D. W. Bertol, E. C. Finardi, A. Sartori, L. H. Meyer, and R. B. Grebogi, "Analysis of training techniques of ANN for classification of insulators in electrical power systems," *IET Gener., Transmiss. Distrib.*, vol. 14, no. 8, pp. 1591–1597, Apr. 2020, doi: 10.1049/iet-gtd.2019.1579.

[47] J. Wang, P. Li, X. Deng, N. Li, X. Xie, H. Liu, and J. Tang, "Evaluation on partial discharge intensity of electrical equipment based on improved ANFIS and ultraviolet pulse detection technology," *IEEE Access*, vol. 7, pp. 126561–126570, 2019, doi: 10.1109/ACCESS.2019.2938784.

[48] T. Yu, J. Yang, and W. Lu, "Dynamic background subtraction using histograms based on fuzzy C-means clustering and fuzzy nearness degree," *IEEE Access*, vol. 7, pp. 14671–14679, 2019, doi: 10.1109/ACCESS.2019.2893771.

[49] S. F. Stefenon, R. Z. Freire, L. H. Meyer, M. P. Corso, A. Sartori, A. Nied, A. C. R. Klaar, and K.-C. Yow, "Fault detection in insulators based on ultrasonic signal processing using a hybrid deep learning technique," *IET Sci., Meas. Technol.*, vol. 14, no. 10, pp. 953–961, Dec. 2020, doi: 10.1049/iet-smt.2020.0083.

STÉFANO FRIZZO STEFENON (Graduate Student Member, IEEE) received the B.E. degree in electrical engineering and the M.E. degree in electrical engineering (power systems) from the Regional University of Blumenau, Brazil, in 2012 and 2015, respectively. He is currently pursuing the Ph.D. degree in electrical engineering (artificial intelligence) with the State University of Santa Catarina, Brazil.

He is also developing research in artificial intelligence applied to the identification of faults in high voltage insulators at the Faculty of Engineering and Applied Science, University of Regina, Canada. His research interests include the classification of insulators, electrical inspections in the distribution networks, and artificial intelligence for fault identification in electrical power systems.

MATHEUS HENRIQUE DAL MOLIN RIBEIRO received the degree in mathematics from the Federal Technological University of Paraná, in 2013, and the M.Sc. degree in biostatistics from the State University of Maringá, in 2015. He is currently pursuing the Ph.D. degree in production and systems engineering with the Pontifical Catholic University of Paraná, Curitiba, Brazil.

He is also an Assistant Professor with the Federal Technological University of Paraná. His research interests include analysis of repeated measures, longitudinal data, statistical models for longitudinal data, time series forecasting, machine learning, and mono and multi-objective optimization.

ADEMIR NIED (Member, IEEE) received the B.E. degree in electrical engineering from the Federal University of Santa Maria, Santa Maria, Brazil, in 1987, the M.S. degree in industrial informatics from the Federal Technological University of Parana, Curitiba, Brazil, in 1995, and the Ph.D. degree in electrical engineering from the Federal University of Minas Gerais, Belo Horizonte, Brazil, in 2007.

Since 1996, he has been a Faculty Member with the State University of Santa Catarina, Joinville, Brazil, where he is currently an Associate Professor with the Department of Electrical Engineering. From 2015 to 2016, he was a Visiting Professor with the Wisconsin Electric Machines and Power Electronics Consortium, University of Wisconsin–Madison, Madison, WI, USA. His teaching and research interests include electrical machines, control of electrical drives, neural networks, and renewable energy.

VIVIANA COCCO MARIANI received the B.E. degree in mathematics from the Federal University of Santa Maria, in 1993, and the master's degree in computer science and the Ph.D. degree in mechanical engineering from the Federal University of Santa Catarina, in 1997 and 2002, respectively.

She is currently a Full Professor with the Department of Mechanical Engineering, Pontifical Catholic University of Paraná (PUCPR), acting as a Professor and an Advisor of the Graduate and Postgraduate Programs in Mechanical Engineering, PUCPR, and an Adjunct Professor with the Federal University of Paraná (UFPR) acting as a Professor with the Department of Electrical Engineering. Her current research interests include regression and classification, with applications in renewable energy problems, such as wind and solar.

LEANDRO DOS SANTOS COELHO received the B.Sc. degree in informatics from the Federal University of Santa Maria, in 1994, the M.Sc. degree in computer science from the Federal University of Santa Catarina, in 1997, the B.Sc. degree in electrical engineering from the Federal University of Santa Maria, in 1999, and the Ph.D. degree in electrical engineering from the Federal University of Santa Catarina, in 2000.

He is currently a Full Professor with the Pontifical Catholic University of Paraná and an Adjunct Professor with the Federal University of Paraná. He is also a member of the Editorial Board of the *Engineering Applications of Artificial Intelligence* (Elsevier), *International Journal of Innovative Computing and Applications*, *International Journal on Power System Optimization*, *Journal of Advanced Research in Evolutionary Algorithms*, *Journal of Engineering*, *The Scientific World Journal*, and *Journal of Advances in Applied & Computational Mathematics*.

VALDERI REIS QUIETINHO LEITHARDT (Member, IEEE) received the Ph.D. degree in computer science from the Federal University of Rio Grande do Sul UFRGS/RS, in 2015.

He is currently an Adjunct Professor with the Polytechnic Institute of Portalegre and a Researcher integrated with the VALORIZA Research Group, School of Technology and Management (ESTG). He is also a collaborating Researcher with the following research groups, such as COPELABS, Universidade Lusófona de Lisboa, Portugal, the IT Branch Covilhã, Telecommunications Institute of Portugal, Portugal, the Department of Informatics, University Beira Interior, Covilhã, Portugal, the Laboratory of Embedded and Distributed Systems, University of Vale do Itajaí (UNIVALI), Brazil, and the Expert Systems and Applications Laboratory, University of Salamanca, Spain. His research interests include distributed systems with a focus on data privacy, communication, and programming protocols, involving scenarios and applications for the Internet of Things, smart cities, big data, cloud computing, and blockchain.

LUIS AUGUSTO SILVA received the degree in internet systems from the Federal Institute of Santa Catarina (IFC), Camboriú, Brazil, in February 2017, and the master's degree in applied computing from the University of Itajaí Valley, Brazil, in 2019. He is currently pursuing the Ph.D. degree in computer engineering with the Universidad de Salamanca, Spain.

His research during his master's degree included the field of notification systems, the IoT, and data privacy. During the master's degree, he was a collaborating Researcher with the Laboratory of Embedded and Distributed Systems (LEDS), UNIVALI, collaborating with research projects related to the Internet of Things. Since August 2020, he has been a Researcher with the Expert Systems and Applications Laboratory (ESALab), Universidad de Salamanca. His research interests include the Internet of Things, embedded drone systems, and data privacy applied to smart environments.

LAIO ORIEL SEMAN received the Ph.D. degree in electrical engineering from the Federal University of Santa Catarina, in 2017.

His research interests include strategies for static and dynamic optimization, along with applications in traffic control, cyber physical systems, and oil and gas production systems.